A&A 551, A136 (2013)
DOI: 10.1051/0004-6361/201220918

Astronomy & Astrophysics

Transition probabilities in Te II and Te III spectra⋆

W. Zhang[1], P. Palmeri[1], P. Quinet[1,2], and É. Biémont[1,2]

[1] Astrophysique et Spectroscopie, Université de Mons – UMONS, Place du Parc 20, 7000 Mons, Belgium
[2] IPNAS (Bât. B15), Université de Liège, Sart Tilman, 4000 Liège, Belgium
e-mail: Patrick.Palmeri@umons.ac.be

Received 14 December 2012 / Accepted 5 February 2013

ABSTRACT

Context. Due to the need of transition probabilities for heavy ions, including those of tellurium, in different fields of physics and in astrophysics, we have investigated theoretically the atomic structure of two selected tellurium ions (Te^{+} and Te^{++}) for which no theoretical data were available so far.
Aims. The first transition probabilities have been calculated for the electric dipole (E1) transitions with wavelengths shorter than 1 micrometer in Te II-III.
Methods. Both the multiconfiguration Dirac-Hartree-Fock (MCDHF) method and the relativistic Hartree-Fock (HFR) approach, in which core-polarization (CPOL) effects were included, have been used for the calculations.
Results. The results obtained with these two completely independent methods are in reasonable agreement. As a consequence, the transition probabilities obtained in this work are expected to be reliable. They fill in a gap concerning the radiative parameters in these two ions.

Key words. atomic data – atomic processes

1. Introduction

Tellurium is important in astrophysics and, more particularly, in stellar nucleosynthesis. In 1973 already, Cowley et al. (1973) were able to obtain abundance estimates for 8 elements in the star HR 465 near the r-process peaks at tellurium and osmium. A large overabundance of tellurium was obtained by assuming that the oscillator strengths were equal to $\log gf = 0.0$, which was obviously a rough approximation imposed by the lack of data on oscillator strengths. Recently, neutral tellurium has been detected by Roederer et al. (2012) in three metal-poor stars (BD + 17 3248, HD 108317, and HD 128279) enriched by products of r-process nucleosynthesis using near-ultraviolet spectra obtained with the Space Telescope Imaging Spectrograph on board the *Hubble* Space Telescope. This element had not been detected previously in Galactic halo stars.

The tellurium ions (Te^{+} and Te^{2+}) have not been identified so far in stellar spectra, one of the obvious reasons being the lack of data on oscillator strengths in these two ions, the results available (Biémont et al. 1995) concerning only the forbidden transitions. Another reason results from the fact that a quantitative analysis of Te II lines is complicated by hyperfine structure effects (Werel & Augustyniak 1981). This lack of radiative data justifies the effort of the present work. It is further motivated by the recent new analysis of Te III spectrum carried out by Tauheed & Naz (2011).

⋆ Tables 8 and 9 are only available in electronic form at the CDS via anonymous ftp to cdsarc.u-strasbg.fr (130.79.128.5) or via http://cdsarc.u-strasbg.fr/viz-bin/qcat?J/A+A/551/A136

2. State-of-the-art analysis of Te II and Te III spectra

The ground configuration of Te II is $5s^25p^3$. The experimentally known even configurations are $5s5p^4$, $5s^25p^2nd$ ($n \geq 5$) and $5s^25p^2ns$ ($n \geq 6$). The excited odd ones are of the types $5s^25p^2np$ ($n \geq 6$) and $5s^25p^2nf$ ($n \geq 4$). The levels compiled in the NIST database (Kramida et al. 2012) are taken from Handrup & Mack (1964) and are characterized by an uncertainty of about 0.2 cm^{-1}. More accurate level values of the ground configuration (uncertainties in the range 0.004–0.007 cm^{-1}) are due to Eriksson (1974). The most recent Te II spectrum analysis is due to Tauheed et al. (2009) but the uncertainties are larger (0.4–2.3 cm^{-1}). The levels considered in the present work have been adopted from the NIST compilation.

Te III belongs to the Sn I isoelectronic sequence and its ground configuration is $5s^25p^2$. The excitation of an outer electron from the ground configuration leads to $5s^25pnd$ ($n \geq 5$) and $5s^25pns$ ($n \geq 6$) while the core excitation gives rise to the $5s5p^3$ configuration. The first investigations of the Te III spectrum are due to Krishnamurty & Rao (1937) and Joshi & Crooker (1964). More recently, the analysis of the Te III spectrum was revised on the basis of configuration interaction calculations by Joshi et al. (1992) but this work was restricted to transitions connecting the ground configuration and $5s^25p5d$, $5s^25p6s$ and $5s5p^3$ configurations. The most recent effort in this ion is due to Tauheed & Naz (2011) who investigated the VUV region (30–200 nm). 150 lines were identified and 60 energy levels were established. The present work is essentially based on this analysis.

The prominent lines of Te II emitted from the ground state configuration ($5s^25p^3$) do appear in the short wavelength range between 79 and 184 nm. In Te III, according to Tauheed & Naz (2011), the lines emitted from the ground $5s^25p^2$

configuration are observed in the 50−75 nm wavelength range. However, Joshi et al. (1992) have observed Te III lines between 77−178 nm.

3. Calculations

A traditional way to obtain transition probabilities in a given ion is to combine lifetime measurements (realized e.g. with a laser spectroscopy technique) with branching fractions deduced either from direct measurements in the laboratory or from atomic structure calculations. When the experimental lifetimes are entirely missing, it is necessary to rely on atomic structure calculations. The accuracy of such calculations is difficult to evaluate particularly in the case of heavy ions or atoms. An interesting information on this accuracy is obtained by comparing calculations realized using several different independent theoretical approaches. The agreement (or disagreement) observed when comparing the different sets of results allows to assess the validity of the theoretical models used. This general procedure was followed in the present work.

3.1. MCDHF calculations in Te II and Te III

A first approach used is the multiconfiguration Dirac-Hartree-Fock (MCDHF) method implemented in the GRASP2K computer package (Jonsson et al. 2007). In this method, the atomic state functions (ASFs), $\Psi(\gamma \mathrm{JM}_J)$, are expanded in linear combinations of configuration state functions (CSFs), $\Phi(\alpha_i \mathrm{JM}_J)$, according to:

$$\Psi(\gamma \mathrm{JM}_J) = \sum_i c_i \Phi(\alpha_i \mathrm{JM}_J). \quad (1)$$

The CSFs are in turn linear combinations of Slater determinants obtained from monoelectronic spin orbitals of the form:

$$\varphi_{n\kappa m}(r,\theta,\phi) = \frac{1}{r}\begin{pmatrix} P_{n\kappa}(r)\chi_{\kappa m}(\theta,\phi) \\ \mathrm{i}Q_{n\kappa}(r)\chi_{-\kappa m}(\theta,\phi) \end{pmatrix}, \quad (2)$$

where $P_{n\kappa}(r)$ and $Q_{n\kappa}(r)$ are, respectively, the large and the small component of the radial wave functions, and the angular functions $\chi_{\kappa m}(\theta,\phi)$ are the spinor spherical harmonics (Grant 1988). The α_i represent all the one-electron and intermediate quantum numbers needed to completely define the CSF. γ is usually chosen as the α_i corresponding to the CSFs with the largest weight $|c_i|^2$. The quantum number κ is given by:

$$\kappa = \pm\left(j + \frac{1}{2}\right), \quad (3)$$

where j is the electron total angular momentum. The sign before the parentheses in Eq. (3) corresponds to the coupling relation between the electron orbital momentum, l, and its spin, i.e.,

$$l = j \pm \frac{1}{2}\cdot \quad (4)$$

The radial functions $P_{n\kappa}(r)$ and $Q_{n\kappa}(r)$ are numerically represented on a logarithmic grid and are required to be orthonormal within each κ symmetry. In the MCDHF variational procedure, the radial functions and the expansion coefficients c_i are optimized to self-consistency.

We have considered the restricted active space (RAS) method for building the MCDHF multiconfiguration expansions. The latter are produced by exciting the electrons from the reference configurations to a given set of orbitals. The rules adopted for generating the configuration space differ according to the correlation model being used. Within a given correlation model, the active set of orbitals spanning the configuration space is increased to monitor the convergence of the total energies and the transition probabilities.

Our calculations have been focused on the E1 transitions $5s^25p^k$–$(5s5p^{k+1} + 5s^25p^{k-1}nl)$ with nl = 5d,6s,6p and k = 3 in Te II and k = 2 in Te III. They have been carried out in six steps for each ion.

In the first step, the core orbitals, i.e. 1s to 4d, together with the 5s and 5p orbitals, have been optimized. All the CSFs (6 in Te II and 5 in Te III) belonging to the ground configuration $5s^25p^k$ were retained in the configuration space. The energy functional was built within the framework of the average level (AL) option (Grant 1988).

The second step consisted in increasing the configuration space by considering all the CSFs (70 in Te II and 41 in Te III) belonging to the following configurations: $5s^25p^k + 5s5p^{k+1} + 5s^25p^{k-1}\{5d,6s,6p\}^1$. The 5d, 6s, and 6p orbitals have been optimized, keeping the others fixed to their values of the first step. The AL option was chosen to build the energy functional.

In the third step, the configuration space has been extended to, respectively, 12 037 in Te II and 4386 in Te III by considering single and double virtual excitations to the active orbital set {5s,5p,5d,6s,6p,6d} from the multi-reference configurations $5s^25p^k + 5s5p^{k+1} + 5s^25p^{k-1}\{5d,6s,6p\}^1$. Only the 6d orbital has been optimized, fixing all the others to the values of the preceding step using an energy functional built from the lowest 70 ASFs in Te II and the lowest 41 ASFs in Te III within the framework of the extended optimal level (EOL) option (Grant 1988). One can note that, from this step of the computation and onward, core-valence and core-core correlations are also considered through single and double excitations of the 5s core electrons, respectively.

The last three steps consisted in extending further the configuration space by adding to the active set of the preceding steps the following orbitals: 7s, 7p, and 7d in the fourth step giving rise to 37 226 CSFs in Te II and 12 812 CSFs in Te III; 8s, 8p, and 8d in the fifth step generating 76 611 CSFs in Te II and 25 802 CSFs in Te III; and finally, 4f in the last step with 102 359 and 32 724 CSFs generated in Te II and Te III, respectively. In these steps, only the added orbitals have been optimized, the others being fixed using the same energy functional as in the third step; also, single and double virtual electron excitations from the same multi-reference configurations as in the third step have been used to generate the configuration spaces. In Te II, further orbital additions to the active set as well as further opening of the core to include more core-valence and core-core correlations have been prevented by the memory limitations of our computer. We did not attempt to extend further our MCDHF calculation in Te III in order to keep a model equivalent to the one used in Te II.

The comparisons between the experimental (Kramida et al. 2012; Tauheed & Naz 2011) and our MCDHF level energies and Landé factors are shown in Tables 1 and 2 for Te II and Te III, respectively. One can notice that the core-excited levels belonging to $5s5p^{k+1}$ have larger deviations from the experimental energies. This may be explained by the missing core-valence and core-core correlations with the opening of the $n \leq 4$ core shells that are implicitly taken into account in our HFR+CPOL calculation through a polarization potential and a fitting procedure (see the next section).

Table 1. Comparison between experimental and MCDHF level energies and Landé factors in Te II.

Designation[a]	E_{DHF}[b] (cm^{-1})	E_{Exp}[a] (cm^{-1})	ΔE[c] (cm^{-1})	g_{DHF}[b]	g_{Exp}[a]	g_{DHF}/g_{Exp}
$5s^25p^3\ ^4S^\circ_{3/2}$	0	0.000	0	1.96	1.93	1.02
$5s^25p^3\ ^2D^\circ_{3/2}$	11 048	10 222.385	826	0.90		
$5s^25p^3\ ^2D^\circ_{5/2}$	13 100	12 421.854	678	1.20		
$5s^25p^3\ ^2P^\circ_{1/2}$	21 496	20 546.591	949	0.67		
$5s^25p^3\ ^2P^\circ_{3/2}$	24 603	24 032.095	571	1.27	1.27	1.00
$5s5p^4(^3P)\ ^4P_{5/2}$	67 933	71 192.526	−3260	1.59	1.59	1.00
$5s5p^4(^3P)\ ^4P_{3/2}$	71 416	74 893.40	−3477	1.72	1.71	1.00
$5s5p^4(^3P)\ ^4P_{1/2}$	72 866	76 300.87	−3435	2.65	2.63	1.01
$5s^25p^2(^3P)6s\ ^4P_{1/2}$	77 595	78 448.22	−853	2.35	2.29	1.02
$5s^25p^2(^3P)5d\ ^2P_{3/2}$	80 856	81 895.43	−1039	1.10	1.12	0.98
$5s^25p^2(^3P)6s\ ^4P_{3/2}$	81 595	82 743.33	−1148	1.50	1.45	1.04
$5s^25p^2(^3P)6s\ ^2P_{3/2}$	82 815	83 577.41	−762	0.98	1.06	0.93
$5s^25p^2(^3P)5d\ ^4F_{5/2}$	84 059	85 049.41	−990	1.11	1.09	1.02
$5s^25p^2(^3P)5d\ ^4F_{3/2}$	84 232	85 159.66	−928	0.81	0.88	0.92
$5s^25p^2(^3P)6s\ ^4P_{5/2}$	84 487	85 591.83	−1105	1.50	1.50	1.00
$5s5p^4(^1D)\ ^2D_{3/2}$	85 447	86 759.90	−1313	0.93	0.94	0.99
$5s5p^4(^1D)\ ^2D_{5/2}$	85 714	87 404.54	−1691	1.23	1.25	0.99
$5s^25p^2(^3P)5d\ ^4F_{7/2}$	86 979	87 899.86	−921	1.26	1.26	1.00
$5s^25p^2(^3P)5d\ ^2P_{1/2}$	87 819	88 796.16	−977	0.38	0.35	1.09
$5s^25p^2(^3P)6s\ ^2P_{3/2}$	87 978	88 961.09	−983	1.19	1.17	1.02
$5s^25p^2(^3P)5d\ ^2F_{5/2}$	88 307	88 924.81	−618	0.95	0.94	1.01
$5s^25p^2(^3P)5d\ ^4F_{9/2}$	89 591	90 519.67	−929	1.32	1.31	1.00
$5s^25p^2(^1D)5d\ ^2F_{7/2}$	90 029	90 797.21	−768	1.27	1.25	1.01
$5s^25p^2(^3P)5d\ ^4D_{3/2}$	91 068	92 191.47	−1123	1.14	1.13	1.00
$5s^25p^2(^3P)5d\ ^4D_{1/2}$	91 605	92 691.51	−1087	0.37	0.42	0.88
$5s^25p^2(^3P)5d\ ^4D_{5/2}$	91 939	92 793.22	−854	1.23	1.24	0.99
$5s^25p^2(^3P)6p\ ^4D^\circ_{1/2}$	93 115	93 978.93	−864	0.84	0.79	1.06
$5s^25p^2(^1D)6s\ ^2D_{5/2}$	94 016	94 860.63	−845	1.26	1.27	0.99
$5s^25p^2(^1D)6s\ ^2D_{3/2}$	94 394	95 208.37	−814	0.96	0.98	0.98
$5s^25p^2(^3P)6p\ ^4D^\circ_{7/2}$	95 213	96 144.74	−932	1.33	1.32	1.00
$5s^25p^2(^3P)5d\ ^4D_{7/2}$	95 668	96 534.6	−867	1.25	1.24	1.01
$5s^25p^2(^3P)6p\ ^2S^\circ_{1/2}$	96 539	97 780.09	−1241	1.21	1.26	0.96
$5s^25p^2(^3P)6p\ ^4S^\circ_{3/2}$	98 484	99 584.59	−1101	1.30	1.26	1.04
$5s^25p^2(^3P)6p\ ^4D^\circ_{5/2}$	98 901	100 112.10	−1211	1.40	1.4	1.00
$5s^25p^2(^3P)6p\ ^2D^\circ_{3/2}$	100 031	101 220.97	−1190	1.26	1.31	0.97
$5s^25p^2(^3P)5d\ ^4P_{5/2}$	100 052	99 229.68	822	1.53	1.51	1.01
$5s^25p^2(^3P)6p\ ^4P^\circ_{1/2}$	100 112	101 370.86	−1259	2.35	2.33	1.01
$5s^25p^2(^1D)5d\ ^2S_{1/2}$	100 528	101 065.37	−537	1.99	2.12	0.94
$5s^25p^2(^1D)5d\ ^2G_{7/2}$	101 082	100 835.8	246	0.94	0.98	0.96
$5s^25p^2(^3P)6p\ ^4P^\circ_{3/2}$	101 273	102 324.49	−1051	1.33	1.31	1.02
$5s^25p^2(^3P)5d\ ^4P_{3/2}$	101 551	100 740.75	810	1.53	1.56	0.98
$5s^25p^2(^3P)6p\ ^4D^\circ_{7/2}$	101 948	103 105.86	−1158	1.39	1.38	1.00
$5s^25p^2(^3P)6p\ ^4P^\circ_{3/2}$	102 681	103 935.90	−1255	1.75	1.74	1.01
$5s^25p^2(^3P)5d\ ^2D_{3/2}$	102 711	102 244.60	466	0.98	0.95	1.03
$5s^25p^2(^3P)5d\ ^4P_{1/2}$	102 764	102 127.22	637	2.42	2.26	1.07
$5s^25p^2(^3P)5d\ ^2D_{5/2}$	103 708	102 703.5	1005	1.10	1.12	0.99
$5s^25p^2(^3P)6p\ ^2P^\circ_{3/2}$	104 065	105 006.08	−941	1.22	1.21	1.01
$5s^25p^2(^3P)6p\ ^2D^\circ_{5/2}$	104 461	105 583.02	−1122	1.29	1.29	1.00
$5s^25p^2(^3P)6p\ ^2P^\circ_{1/2}$	105 086	106 119.20	−1033	0.86	0.87	0.99
$5s^25p^2(^1S)6s\ ^2S_{1/2}$	108 090	109 005.8	−916	1.70		
$5s^25p^2(^3P)5d\ ^2F_{7/2}$	108 210	107 244.4	966	1.12	1.19	0.94
$5s^25p^2(^1D)5d\ ^2P_{1/2}$	108 768	107 521.8	1246	1.14		
$5s^25p^2(^1D)5d\ ^2F_{5/2}$	109 538	108 819.4	719	1.01		
$5s^25p^2(^3P)6p\ ^2D^\circ_{5/2}$	110 944	111 946.69	−1003	1.19	1.19	1.00
$5s^25p^2(^1D)5d\ ^2P_{3/2}$	111 177	110 136.3	1041	1.34		
$5s^25p^2(^1D)6p\ ^2D^\circ_{3/2}$	111 303	112 272.43	−969	1.05	1.09	0.96
$5s^25p^2(^1D)6p\ ^2F^\circ_{5/2}$	111 690	112 548.84	−859	1.02	1.06	0.96
$5s^25p^2(^1D)6p\ ^2F^\circ_{7/2}$	111 934	112 788.49	−854	1.19	1.20	0.99
$5s^25p^2(^1D)6p\ ^2P^\circ_{1/2}$	113 287	114 068.52	−782	0.74	0.77	0.96
$5s^25p^2(^1D)5d\ ^2D_{3/2}$	114 014	111 856.1	2158	0.90		
$5s^25p^2(^1D)5d\ ^2D_{5/2}$	114 884	113 564.5	1320	1.21		
$5s^25p^2(^1D)6p\ ^2P^\circ_{3/2}$	115 288	116 101.71	−814	1.28	1.29	1.00
$5s^25p^2(^1S)5d\ ^2D_{3/2}$	119 058	118 325.5	733	0.80		
$5s^25p^2(^1S)5d\ ^2D_{5/2}$	119 587	118 420.6	1166	1.19		
$5s5p^4(^3P)\ ^2P_{1/2}$	119 885	117 192.38	2693	1.04		
$5s^25p^2(^1S)6p\ ^2P^\circ_{1/2}$	125 147	126 047.99	−901	0.67	0.29	2.30
$5s^25p^2(^1S)6p\ ^2P^\circ_{3/2}$	125 844	126 309.55	−466	1.33	1.02	1.31

Notes. [a] Kramida et al. (2012); [b] MCDHF (this work); [c] $\Delta E = E_{DHF} - E_{Exp}$.

Table 2. Comparison between experimental and MCDHF level energies and Landé factors in Te III.

Designation[a]	E_{DHF}[b] (cm^{-1})	E_{Exp}[a] (cm^{-1})	ΔE[c] (cm^{-1})	g_{DHF}[b]	g_{Exp}[d]	g_{DHF}/g_{Exp}
$5s^25p^2\ ^3P_0$	0	0.0	0			
$5s^25p^2\ ^3P_1$	4401	4757.2	−356	1.50		
$5s^25p^2\ ^3P_2$	7824	8167.0	−343	1.41		
$5s^25p^2\ ^1D_2$	17 057	17 359.8	−303	1.10		
$5s^25p^2\ ^1S_0$	30 491	30 398.3	93			
$5s5p^3(^4S)\ ^5S^\circ_2$	58 842	64 586.5	−5745	1.99		
$5s5p^3(^2D)\ ^3D^\circ_1$	79 119	82 889.1	−3770	0.56		
$5s5p^3(^2D)\ ^3D^\circ_2$	79 406	83 203.4	−3797	1.20		
$5s5p^3(^2D)\ ^3D^\circ_3$	81 273	85 205.6	−3933	1.33		
$5s5p^3(^2P)\ ^3P^\circ_2$	92 185	95 031.3	−2846	1.26		
$5s5p^3(^2P)\ ^3P^\circ_0$	92 930	96 061.6	−3132			
$5s5p^3(^2P)\ ^3P^\circ_1$	93 431	96 581.5	−3151	1.45		
$5s5p^3(^2P)\ ^3P^\circ_2$	97 488	100 469.1	−2981	1.18	1.13	1.04
$5s^25p5d\ ^3F^\circ_2$	102 882	104 717.2	−1835	0.72		
$5s^25p5d\ ^3F^\circ_3$	104 644	106 314.8	−1671	1.09	1.07	1.02
$5s^25p6s\ ^3P^\circ_0$	105 878	107 470.0	−1592			
$5s^25p6s\ ^3P^\circ_1$	106 374	107 726.6	−1353	1.37	1.37	1.00
$5s^25p5d\ ^3P^\circ_2$	113 858	115 422.2	−1564	1.49	1.28	1.16
$5s^25p5d\ ^1P^\circ_0$	113 901	114 216.4	−315	1.07	1.00	1.07
$5s^25p6s\ ^3P^\circ_2$	117 392	116 719.4	673	1.34	1.34	1.00
$5s^25p5d\ ^3D^\circ_1$	117 444	115 747.6	1696	0.84		
$5s^25p6s\ ^1P^\circ_1$	119 993	117 796.1	2197	1.33	1.26	1.06
$5s^25p5d\ ^1F^\circ_3$	121 689	120 903.4	786	1.30	1.35	0.96
$5s^25p5d\ ^3P^\circ_0$	122 998	122 541.0	457			
$5s^25p5d\ ^3P^\circ_1$	123 047	122 127.4	920	1.24		
$5s^25p5d\ ^3D^\circ_2$	123 476	122 515.0	961	1.29		
$5s^25p5d\ ^3P^\circ_1$	126 627	124 787.9	1839	1.62		
$5s^25p6p\ ^3D_1$	126 865	128 617.9	−1753	0.72	0.68	1.06
$5s^25p5d\ ^3F^\circ_3$	128 502	127 242.3	1260	1.03		
$5s^25p6p\ ^3P^\circ_1$	130 258	132 116.7	−1859	1.27	1.24	1.03
$5s5p^3(^2D)\ ^1D^\circ_2$	130 315	127 188.8	3126	1.04		
$5s^25p6p\ ^3P_0$	130 575	132 262.4	−1687			
$5s^25p6p\ ^3D_2$	130 598	132 329.1	−1731	1.19	1.16	1.03
$5s^25p6p\ ^1P_1$	136 083	138 289.7	−2207	1.14	1.02	1.12
$5s^25p6p\ ^3P_2$	137 599	139 664.5	−2066	1.36	1.43	0.95
$5s^25p6p\ ^3D_3$	138 061	139 949.7	−1889	1.33	1.28	1.04
$5s^25p6p\ ^3S_1$	139 694	141 803.0	−2109	1.87	1.76	1.06
$5s5p^3(^2P)\ ^1P^\circ_1$	139 847	136 476.2	3371	1.03		
$5s^25p6p\ ^1D_2$	141 021	142 982.0	−1961	1.12	1.14	0.98

Notes. [a] Tauheed & Naz (2011). 5p6p levels are from Kramida et al. (2012). The first component of the LS composition by Tauheed & Naz (2011) is taken as the designation. [b] MCDHF (this work). [c] $\Delta E = E_{DHF} - E_{Exp}$. [d] Kramida et al. (2012).

The final MCDHF electric dipole (E1) transition probabilities have been corrected using the experimental energies as follows:

$$A_{ki}^{cor} = \left(\frac{E_k^{exp} - E_i^{exp}}{E_k^{DHF} - E_i^{DHF}} \right)^3 A_{ki}^{DHF} \quad (5)$$

where A_{ki}^{cor} and A_{ki}^{DHF} are respectively the corrected and MCDHF transition probability of the E1 transition between the upper level k and the lower level i, and $E_{k(i)}^{exp}$ and $E_{k(i)}^{DHF}$ are respectively the experimental and the MCDHF upper (lower) level energy.

These A-values have been determined in the Babushkin and Coulomb gauges, the equivalents of the length and velocity gauges in the non-relativistic limit. A good agreement between these values is a necessary condition for an accurate estimate of the line strength, though it is still not a sufficient condition. We have therefore considered an additional and independent criteria to estimate this accuracy; we have modified the GRASP2K package (Jonsson et al. 2007) to include the calculation of the cancellation factor (CF) as defined by Cowan (1981), i.e.:

$$CF = \left(\frac{|\sum_k \sum_i c'_k < \Phi'(\alpha_k J M_J)|D^{(1)}|\Phi(\alpha_i J M_J) > c_i|}{\sum_i \sum_k |c'_k < \Phi'(\alpha_k J M_J)|D^{(1)}|\Phi(\alpha_i J M_J) > c_i|} \right)^2 \quad (6)$$

where $D^{(1)}$ is the electric dipole operator and $c_{i(k)}(')$ and $\Phi(')(\alpha_{i(k)} J M_J)$ have the same meanings as in Eq. (1) for the initial (non-primed symbols) and final (primed symbols) states of the transition. A small value of the cancellation factor (say less than 0.05) indicates that the calculated line strength is affected by a strong cancellation effect; this is due to opposite sign contributions of almost equal and significant amplitudes that cancel each other in the transition amplitude expansions which are directly related to the ASF representation (here, in jj coupling). Table 3 illustrates in Te II the complementarity of the gauges agreement criteria and the cancellation factor in the four possible cases, i.e. bad gauges agreement (agreement >10%) and small

Table 3. Illustration in Te II of the complementarity between the criteria of the gauges agreement and the cancellation factor in the estimation of the A-value accuracy in the four possible cases.

Transition	MCDHF			HFR+CPOL	
	$gA_B(s^{-1})^a$	C/B^b	CF	$gA(s^{-1})$	CF
$5s^25p^3\ {}^4S^\circ_{3/2}-5s^25p^2(^1D)5d\ {}^2F_{5/2}$	2.29(+6)	0.66	2(−5)	6.51(+7)	6(−3)
$5s^25p^2(^1D)5d\ {}^2S_{1/2}-5s^25p^2(^1D)6p\ {}^2P^\circ_{1/2}$	2.70(+7)	0.56	0.15	6.15(+6)	0.22
$5s^25p^2(^3P)5d\ {}^2P_{1/2}-5s^25p^2(^3P)6p\ {}^2S^\circ_{1/2}$	1.60(+6)	1.04	0.04	1.83(+6)	0.08
$5s^25p^2(^3P)6s\ {}^4P_{1/2}-5s^25p^2(^3P)6p\ {}^4D^\circ_{3/2}$	3.29(+8)	0.96	0.63	3.06(+8)	0.64

Notes. Only the last transition is to be retained in the MCDHF calculation. The corresponding HFR+CPOL transition probabilities and CF values are listed for comparison. $^{(a)}$ Babushkin gauge corrected using the experimental level energies. $^{(b)}$ Coulomb to Babushkin ratio. $A(B)$ stands for $A \times 10^B$.

CF(<0.05), bad gauges agreement and $CF > 0.05$, good gauges agreement (agreement <10%) and small CF, and good gauges agreement and $CF > 0.05$; only the last case is indicative of an accurate MCDHF A-value. The corresponding HFR+CPOL transition probabilities and CF values have been also included for comparison.

3.2. Relativistic Hartree-Fock (HFR)

The relativistic Hartree-Fock (HFR) approach including core-polarization (CPOL) effects by means of a model potential and a correction to the transition dipole operator (HFR + CPOL) have been used to investigate the transition probabilities of Te II and Te III.

For Te II, 43 configurations: $5p^3 + 5p^26p + 5p^27p + 5p^24f + 5p^25f + 5p^26f + 5d^26p + 5d^26f + 6s^27p + 5d^27p + 4f^25p + 5f^26p + 5s5p^36s + 5s5p^35d + 5s5p^36d + 5s5p^26p5d + 5s5p^26p6d + 5s5p^24f5d + 5s5p^24f6d + 5p^5$ (odd parity) and $5s5p^4 + 5p^25d + 5p^26d + 5p^27d + 5p^26d + 5p^27d + 5p^26s + 5p^27s + 5p^28s + 5p^25g + 5p^26g + 5d^25g + 5d^26g + 5f^25g + 5f^26g + 5s5p^36p + 5s5p^34f + 5s5p^35f + 5s5p^36f + 5s5p^26s5d + 5s5p^26s6d + 5s5p^25d6d + 5s5p^26s^2 + 5s5p^25d^2$ (even parity) have been considered.

For Te III, 48 configurations: $5p^2 + 5p6p + 5p7p + 5p4f + 5p5f + 5p6f + 5d6s + 5d6d + 6s^2 + 5d^2 + 4f^2 + 5f^2 + 5s5p^26s + 5s5p^25d + 5s5p^26d + 5s5p6s6p + 5s5p6p5d + 5s5p6p6d + 5s5p4f5d + 5s5p4f6d + 5p^4 + 5p^34f + 5p^35f + 5p^36f$ (even parity) and $5s5p^3 + 5p5d + 5p6d + 5p7d + 5p6s + 5p7s + 5p8s + 5p5g + 5p6g + 5d6p + 5d4f + 5d5f + 5d6f + 5s5p^26p + 5s5p^24f + 5s5p^25f + 5s5p^26f + 5s5p6s5d + 5s5p6s6d + 5s5p5d6d + 5s5p6s^2 + 5s5p5d^2 + 5p^36s + 5p^35d + 5p^36d$ (odd parity) were included in the calculations.

In order to consider the CPOL corrections in Te II and Te III calculations, a dipole polarizability of $\alpha_d = 1.295a_0^3$ and a cut-off radius of $r_c = 0.964\ a_0$ were adopted. Some radial integrals, considered as free parameters, were then adjusted with a least-squares optimization program minimizing the discrepancies between the calculated Hamiltonian eigenvalues and the experimental energy levels. More precisely, the average energies (E_{av}), the electrostatic direct (F^k) and exchange (G^k) integrals, the spin-orbit (ζ_{nl}) and effective interaction (α) parameters were allowed to vary during the fitting process. The scaling factors, i.e. the ratios between the fitted and the HFR values (LSF/HFR), of the optimized parameters ranged between 0.61 to 1.04, 0.50 to 1.19 and 0.85 to 1.19 for, respectively, the F^k, G^k and ζ_{nl} integrals in Te II. In Te III, these scaling factors became $0.72 \le$ LSF/HFR(F^k) ≤ 0.93, $0.62 \le$ LSF/HFR(G^k) ≤ 0.95 and $0.86 \le$ LSF/HFR(ζ_{nl}) ≤ 1.27.

For Te II, the energy levels calculated with the HFR+CPOL method are compared to available experimental values in Tables 4 (odd levels) and 5 (even levels), the mean deviations of the fits being found equal to 217 cm^{-1} (81 levels, 36 parameters) for the even parity and 87 cm^{-1} (45 levels, 19 parameters) for the odd parity. For Te III, the results of the energy levels are included in Tables 6 (even levels) and 7 (odd levels), the mean deviations reaching 100 and 126 cm^{-1} for even and odd parity (for the even parity, 14 levels, 9 parameters; for the odd parity, 55 levels, 27 parameters), respectively. The lowest unknown energy levels, i.e. $5s^25p^2(^1D)5d\ {}^2G_{9/2}$ in Te II and $5s^25p5d\ {}^3F^o_4$ in Te III, are also given in Tables 5 and 7.

The weighted oscillator strengths ($\log gf$) and transition probabilities (gA) (HFR + CPOL calculations) are reported in Tables 8 (Te II) and 9 (Te III). The electric dipole (E1) transitions between the levels reported in Tables 5–7 with wavelengths less than 1 micrometer and with cancellation factors greater than 0.05 have been selected. In Te II, the list of reported transitions has been further limited to those having a $\log gf > -1$. No limit in log gf has been set in Te III. This represents a total number of 439 transitions for Te II and 284 for Te III. Some of these transitions are emitted from high energy levels (>8 eV) and have no chance to be observed in astrophysics. Nevertheless, they are kept in the tables for completion. There are no other (experimental or theoretical) transition probabilities available for comparison.

A majority of the calculated energy levels of Te II obtained with the HFR + CPOL method are strongly mixed, the average LS-purities being equal to 56% and 53% for the odd and even parities, respectively. For Te III, many calculated energy levels are strongly mixed and the average LS-purities of the calculated energy levels obtained by the HFR + CPOL method are equal to 74% and 65% for the even and odd parities, respectively. According to our level LS-compositions in Te III, those given in Tauheed & Naz (2011) should be swapped between the odd levels with $J = 2$ located at 115 422.2 cm^{-1} and at 116 719.4 cm^{-1}, and between the odd levels with $J = 3$ located at 120 903.4 cm^{-1} and at 127 242.3 cm^{-1}. Moreover, the first LS-component of the odd levels with $J = 3$ situated at 120 903.4 cm^{-1} is $5s^25p5d\ {}^3D^o_3$ and not $5s^25p5d\ {}^3F^o_3$ as this last spectroscopic term appears twice with purities close to 90% in the matrix $J = 3$ given in the Table 2 of Tauheed & Naz (2011); this was actually a typo as the correct designation was already given in Joshi et al. (1992). Concerning the swapping of designations between the two above-mentioned $J = 2$ odd levels, although there is an agreement between Tauheed & Naz (2011) and Joshi et al. (1992), our HFR+CPOL designations agree with the NIST database (Kramida et al. 2012) and there is a consistancy with our MCDHF, HFR+CPOL and the experimental Landé g factors (we took the Tauheed & Naz (2011) designations in Table 2 as our MCDHF calculation is in jj-coupling

Table 4. Comparison between experimental and HFR+CPOL level energies and Landé factors in Te II (odd levels).

E_{Exp} [a] (cm^{-1})	E_{Calc} [b] (cm^{-1})	g_{Calc} [b]	g_{Exp} [a]	g_{Calc}/g_{Exp}	LS-composition[b]
$J = 1/2$					
20 546.591	20 566	0.67			96.8% $5s^25p^3\ ^2P^\circ$ + 1.6% $5p^5\ ^2P^\circ$
93 978.93	94 001	0.80	0.79	1.01	49.5% $5p^2(^3P)6p\ ^4D^\circ$ + 21.0% $5p^2(^3P)6p\ ^2S^\circ$
97 780.09	97 809	1.26	1.26	1.00	48.6% $5p^2(^3P)6p\ ^2S^\circ$ + 38.0% $5p^2(^3P)6p\ ^4D^\circ$
101 370.86	101 204	2.33	2.33	1.00	74.8% $5p^2(^3P)6p\ ^4P^\circ$ + 10.1% $5p^2(^3P)6p\ ^2P^\circ$
106 119.20	106 214	0.85	0.87	0.98	71.4% $5p^2(^3P)6p\ ^2P^\circ$ + 11.9% $5p^2(^3P)6p\ ^2S^\circ$
114 068.52	113 939	0.76	0.77	0.98	86.3% $5p^2(^1D)6p\ ^2P^\circ$ + 5.0% $5p^2(^3P)6p\ ^2S^\circ$
125 287.32	125 295	0.84	0.86	0.98	25.7% $5p^2(^1S)6p\ ^2P^\circ$ + 32.3% $5p^2(^3P)4f\ ^4D^\circ$
126 047.99	126 080	0.53	0.29	1.83	46.9% $5p^2(^3P)4f\ ^4D^\circ$ + 31.9% $5p^2(^1S)6p\ ^2P^\circ$
$J = 3/2$					
0.000	2	1.94	1.93	1.01	89.9% $5s^25p^3\ ^4S^\circ$ + 6.4% $5s^25p^3\ ^2P^\circ$
10 222.385	10 185	0.93			79.4% $5s^25p^3\ ^2D^\circ$ + 13.9% $5s^25p^3\ ^2P^\circ$
24 032.095	24 014	1.27	1.27	1.00	76.5% $5s^25p^3\ ^2P^\circ$ + 16.8% $5s^25p^3\ ^2D^\circ$
96 144.74	96 138	1.34	1.32	1.02	48.8% $5p^2(^3P)6p\ ^4D^\circ$ + 22.1% $5p^2(^3P)6p\ ^4P^\circ$
99 584.59	99 618	1.32	1.26	1.05	41.3% $5p^2(^3P)6p\ ^4D^\circ$ + 16.2% $5p^2(^3P)6p\ ^2D^\circ$
101 220.97	101 295	1.24	1.31	0.94	51.8% $5p^2(^3P)6p\ ^2D^\circ$ + 27.5% $5p^2(^3P)6p\ ^4S^\circ$
103 935.90	103 702	1.73	1.74	0.99	41.6% $5p^2(^3P)6p\ ^4P^\circ$ + 36.3% $5p^2(^3P)6p\ ^4S^\circ$
105 006.08	105 021	1.21	1.21	1.00	60.9% $5p^2(^3P)6p\ ^2P^\circ$ + 24.8% $5p^2(^1D)6p\ ^2D^\circ$
112 272.43	112 161	1.09	1.09	1.00	45.1% $5p^2(^1D)6p\ ^2D^\circ$ + 24.4% $5p^2(^1D)6p\ ^2P^\circ$
116 101.71	116 022	1.28	1.29	0.99	49.3% $5p^2(^1D)6p\ ^2P^\circ$ + 20.4% $5p^2(^3P)6p\ ^2P^\circ$
122 775.20	122 749	0.72	0.71	1.01	46.7% $5p^2(^3P)4f\ ^4F^\circ$ + 25.1% $5p^2(^3P)4f\ ^4D^\circ$
125 442.46	125 337	1.21	1.21	1.00	29.7% $5p^2(^1S)6p\ ^2P^\circ$ + 24.4% $5p^2(^3P)4f\ ^4D^\circ$
126 138.35	126 087	0.87	0.91	0.96	31.9% $5p^2(^3P)4f\ ^4F^\circ$ + 26.4% $5p^2(^3P)4f\ ^4D^\circ$
126 309.55	126 374	1.06	1.02	1.04	35.3% $5p^2(^3P)4f\ ^2D^\circ$ + 34.6% $5p^2(^1S)6p\ ^2P^\circ$
$J = 5/2$					
12 421.854	12 455	1.20			97.4% $5s^25p^3\ ^2D^\circ$ + 0.8% $5s5p^35d\ ^2D^\circ$
100 112.10	100 114	1.40	1.40	1.00	76.9% $5p^2(^3P)6p\ ^4D^\circ$ + 15.0% $5p^2(^3P)6p\ ^4P^\circ$
102 324.49	102 316	1.33	1.31	1.03	34.3% $5p^2(^3P)6p\ ^4P^\circ$ + 23.5% $5p^2(^3P)6p\ ^2D^\circ$
105 583.02	105 731	1.27	1.29	0.98	45.4% $5p^2(^3P)6p\ ^2D^\circ$ + 29.3% $5p^2(^3P)6p\ ^4P^\circ$
111 946.69	111 831	1.23	1.19	1.04	63.6% $5p^2(^1D)6p\ ^2D^\circ$ + 17.9% $5p^2(^3P)6p\ ^4P^\circ$
112 548.84	112 770	1.01	1.06	0.95	58.8% $5p^2(^1D)6p\ ^2F$ + 22.4% $5p^2(^3P)6p\ ^2D$
117 685.83	117 721	0.84	0.85	0.99	46.0% $5p^2(^3P)4f\ ^4G^\circ$ + 17.8% $5p^2(^3P)4f\ ^2D^\circ$
122 027.77	121 975	0.95	0.95	1.00	41.2% $5p^2(^3P)4f\ ^4G^\circ$ + 38.8% $5p^2(^3P)4f\ ^2D^\circ$
122 887.62	122 871	1.18	1.16	1.02	38.4% $5p^2(^3P)4f\ ^4D^\circ$ + 18.8% $5p^2(^3P)4f\ ^2F^\circ$
123 885.43	123 890	1.40	1.38	1.01	62.8% $5p^2(^3P)7p\ ^4D^\circ$ + 22.9% $5p^2(^3P)7p\ ^4P^\circ$
126 063.01	125 955	1.10	1.11	0.99	45.7% $5p^2(^3P)4f\ ^4F^\circ$ + 23.4% $5p^2(^3P)4f\ ^4D^\circ$
126 219.97	126 287	0.94	0.97	0.97	51.7% $5p^2(^3P)4f\ ^2F^\circ$ + 17.3% $5p^2(^1D)4f\ ^2F^\circ$
135 403.3	135 471	1.18			70.9% $5p^2(^1D)4f\ ^2D^\circ$ + 9.3% $5p^2(^3P)4f\ ^4D^\circ$
$J = 7/2$					
103 105.86	103 111	1.38	1.38	1.00	79.9% $5p^2(^3P)6p\ ^4D^\circ$ + 16.6% $5p^2(^1D)6p\ ^2F^\circ$
112 788.49	112 998	1.19	1.20	0.99	80.3% $5p^2(^1D)6p\ ^2F^\circ$ + 16.2% $5p^2(^3P)6p\ ^4D^\circ$
117 859.06	117 892	1.15	1.13	1.02	26.4% $5p^2(^3P)4f\ ^4D^\circ$ + 20.3% $5p^2(^3P)4f\ ^4G^\circ$
122 137.90	122 077	1.20	1.18	1.02	47.2% $5p^2(^3P)4f\ ^4D^\circ$ + 36.3% $5p^2(^3P)4f\ ^4G^\circ$
122 616.65	122 715	0.98	0.98	1.00	52.1% $5p^2(^3P)4f\ ^2G^\circ$ + 24.7% $5p^2(^3P)4f\ ^4G^\circ$
125 983.78	125 887	1.15	1.20	0.96	48.6% $5p^2(^3P)4f\ ^4F^\circ$ + 16.5% $5p^2(^1D)4f\ ^2G^\circ$
126 164.22	126 166	1.10	1.12	0.98	49.3% $5p^2(^3P)4f\ ^2F^\circ$ + 17.5% $5p^2(^1D)4f\ ^2G^\circ$
$J = 9/2$					
122 427.00	122 487	1.21	1.25	0.97	57.6% $5p^2(^3P)4f\ ^4G^\circ$ + 25.2% $5p^2(^3P)4f\ ^4F^\circ$
125 644.34	125 622	1.18	1.19	0.99	30.6% $5p^2(^3P)4f\ ^4F^\circ$ + 25.9% $5p^2(^3P)4f\ ^4G^\circ$
$J = 11/2$					
125 495.39	125 563	1.24	1.31	0.94	77.5% $5p^2(^3P)4f\ ^4G^\circ$ + 19.5% $5p^2(^1D)4f\ ^2H^\circ$

Notes. [(a)] Kramida et al. (2012). [(b)] HFR + CPOL (this work).

but the experimental Landé g factors follow the NIST database designations which agree with our HFR+CPOL calculation). In addition, it appears that it is actually the ab initio HFR order using both the CI considered in Tauheed & Naz (2011) and our more extended CI expansion.

4. Discussion

The comparisons between the MCDHF and HFR+CPOL $\log gf$ in Te II and Te III are given in Figs. 1 and 2 respectively; only transitions with a gauge agreement better than 10% and $CF > 0.05$ (in both MCDHF and HFR+CPOL) have been retained. In Te II, the average oscillator strength ratio between HFR+CPOL and MCDHF is 0.99 ± 0.31 (where the second number is the standard deviation) for $\log gf$(HFR+CPOL) ≥ −1 suggesting an accuracy of about 60% (two times the standard deviation) for the strong lines reported in Table 8. Concerning Te III, this ratio becomes 1.21 ± 0.80 due to essentially a few (9 on a total of 65 lines) transitions that present strong disagreements between MCDHF and HFR+CPOL (factor two and more)

Table 5. Comparison between experimental and HFR+CPOL level energies and Landé factors in Te II (even levels).

E_{Exp}[a] (cm^{-1})	E_{Calc}[b] (cm^{-1})	g_{Calc}[b]	g_{Exp}[a]	g_{Calc}/g_{Exp}	LS-composition[b]
$J = 1/2$					
76 300.87	76 414	2.63	2.63	1.00	66.7% 5s5p^4(^{3}P) ^{4}P + 17.7% 5p^2(^{3}P)5d ^{4}P
78 448.22	78 364	2.28	2.29	1.00	65.1% 5p^2(^{3}P)6s ^{4}P + 15.7% 5p^2(^{3}P)6s ^{2}P
83 577.41	83 286	1.07	1.06	1.01	63.4% 5p^2(^{3}P)6s ^{2}P + 18.8% 5p^2(^{3}P)6s ^{4}P
88 796.16	88 585	0.39	0.35	1.11	44.2% 5p^2(^{3}P)5d ^{4}D + 32.8% 5p^2(^{3}P)5d ^{2}P
92 691.51	92 425	0.37	0.42	0.88	50.7% 5p^2(^{3}P)5d ^{4}D + 32.2% 5p^2(^{3}P)5d ^{2}P
101 065.37	100 578	2.16	2.12	1.02	43.4% 5p^2(^{1}D)5d ^{2}S + 19.3% 5p^2(^{3}P)5d ^{4}P
102 127.22	102 377	2.30	2.26	1.02	49.9% 5p^2(^{3}P)5d ^{4}P + 13.2% 5p^2(^{1}D)5d ^{2}S
107 521.8	108 077	1.31			48.8% 5p^2(^{1}D)5d ^{2}P + 34.5% 5p^2(^{1}S)6s ^{2}S
109 005.8	109 284	1.50			42.4% 5p^2(^{1}S)6s ^{2}S + 29.9% 5p^2(^{1}D)5d ^{2}P
112 823.93	112 877	2.23	2.16	1.03	73.0% 5p^2(^{3}P)7s ^{4}P + 16.3% 5p^2(^{3}P)7s ^{2}P
117 192.38	116 980	0.99			31.0% 5s5p^4(^{3}P) ^{2}P + 26.6% 5p^2(^{3}P)6d ^{2}P
118 009.02	118 319	1.10	1.16	0.95	71.0% 5p^2(^{3}P)7s ^{2}P + 19.9% 5p^2(^{3}P)7s ^{4}P
121 106.21	121 239	0.48	0.52	0.92	72.9% 5p^2(^{3}P)6d ^{4}D + 5.9% 5s5p^4(^{1}S) ^{2}S
123 657.46	123 709	1.35	1.15	1.17	27.9% 5s5p^4(^{1}S) ^{2}S + 15.2% 5p^2(^{3}P)6d ^{2}P
125 477.6	125 286	2.38			73.0% 5p^2(^{3}P)6d ^{4}P + 5.6% 5s5p^4(^{1}S) ^{2}S
126 212.00	126 144	2.06	2.03	1.01	64.1% 5p^2(^{3}P)8s ^{4}P + 26.5 5p^2(^{3}P)8s ^{2}P
128 082.5	128 374	0.85			30.2% 5p^2(^{3}P)6d ^{2}P + 20.4% 5p^2(^{3}P)7d ^{2}P
134 123.7	134 153	0.74			64.0% 5p^2(^{1}D)6d ^{2}P + 11.4% 5p^2(^{3}P)7d ^{2}P
136 889.5	136 501	1.20			38.5% 5p^2(^{3}P)7d ^{2}P + 31.5% 5p^2(^{1}D)6d ^{2}S
141 894.6	141 420	2.00			88.1% 5p^2(^{1}S)7s ^{2}S + 4.5% 5p^2(^{3}P)7s ^{4}P
$J = 3/2$					
74 893.40	74 913	1.71	1.71	1.00	74.0% 5s5p^4(^{3}P) ^{4}P + 18.8% 5p^2(^{3}P)5d ^{4}P
81 895.43	81 721	1.22	1.12	1.09	28.3% 5p^2(^{3}P)5d ^{2}P + 22.8% 5p^2(^{3}P)6s ^{4}P
82 743.33	82 709	1.46	1.45	1.01	65.9% 5p^2(^{3}P)6s ^{4}P + 12.5% 5p^2(^{3}P)5d ^{4}F
85 159.66	85 102	0.81	0.88	0.92	54.6% 5p^2(^{3}P)5d ^{4}F + 22.3% 5p^2(^{3}P)5d ^{2}P
86 759.90	86 713	0.92	0.94	0.98	27.2% 5s5p^4(^{1}D) ^{2}D + 24.3% 5p^2(^{1}D)5d ^{2}D
88 961.09	88 944	1.17	1.17	1.00	31.2% 5p^2(^{3}P)6s ^{2}P + 22.8% 5p^2(^{3}P)5d ^{4}D
92 191.47	92 177	1.13	1.13	1.00	57.9% 5p^2(^{3}P)5d ^{4}D + 9.6% 5s5p^4(^{1}D) ^{2}D
95 208.37	95 263	0.95	0.98	0.97	61.3% 5p^2(^{1}D)6s ^{2}D + 21.6% 5p^2(^{3}P)6s ^{2}P
100 740.75	100 685	1.60	1.56	1.03	60.9% 5p^2(^{3}P)5d ^{4}P + 13.0% 5s5p^4(^{3}P) ^{4}P
102 244.60	102 377	0.90	0.95	0.96	60.1% 5p^2(^{3}P)5d ^{2}D + 8.8% 5p^2(^{1}S)5d ^{2}D
110 136.3	110 045	1.29			56.8% 5p^2(^{1}D)5d ^{2}P + 20.5% 5s5p^4(^{3}P) ^{2}P
111 856.1	112 026	0.97			38.9% 5p^2(^{1}D)5d ^{2}D + 20.4% 5s5p^4(^{1}D) ^{2}D
115 700.56	115 643	0.95	0.91	1.04	23.4% 5p^2(^{3}P)6d ^{4}F + 23.9% 5p^2(^{3}P)6d ^{2}P
117 264.02	117 417	1.23	0.98	1.26	39.1% 5p^2(^{3}P)7s ^{4}P + 18.1% 5p^2(^{3}P)6d ^{4}F
117 339.70	117 273	1.34	1.60	1.54	51.1% 5p^2(^{3}P)7s ^{4}P + 13.6% 5p^2(^{3}P)6d ^{4}F
118 325.5	118 325	0.78			48.6% 5p^2(^{1}S)5d ^{2}D + 16.0% 5p^2(^{3}P)6d ^{4}F
121 173.94	121 673	1.21	1.23	0.98	33.8% 5p^2(^{3}P)7s ^{2}P + 27.2% 5p^2(^{3}P)6d ^{4}D
121 518.93	121 285	1.21	1.20	1.01	30.0% 5p^2(^{3}P)7s ^{2}P + 23.2% 5p^2(^{3}P)6d ^{4}D
124 082.07	124 389	1.09	1.10	0.99	18.7% 5p^2(^{3}P)6d ^{2}P + 16.3% 5p^2(^{3}P)6d ^{2}D
125 066.06	124 865	1.50	1.52	0.99	55.1% 5p^2(^{3}P)6d ^{4}P + 21.6% 5p^2(^{3}P)6d ^{4}D
126 516.86	126 645	0.99	0.98	1.01	25.9% 5p^2(^{3}P)6d ^{2}D + 19.9% 5p^2(^{3}P)6d ^{2}P
129 789.2	129 999	1.08			58.4% 5p^2(^{1}D)7s ^{2}D + 16.7% 5p^2(^{3}P)7s ^{2}P
134 495.3	134 814	1.07			37.9% 5p^2(^{1}D)6d ^{2}D + 11.7% 5p^2(^{3}P)7d ^{4}P
135 582.2	135 600	0.93			34.0% 5p^2(^{3}P)7d ^{2}D + 28.4 % 5p^2(^{1}D)6d ^{2}D
147 105.3	147 607	0.80			88.8% 5p^2(^{1}S)6d ^{2}D + 2.8% 5p^2(^{3}P)6d ^{2}D
$J = 5/2$					
71 192.526	71 157	1.59	1.59	1.00	76.3% 5s5p^4(^{3}P) ^{4}P + 16.8% 5p^2(^{3}P)5d ^{4}P
85 049.41	85 283	1.10	1.09	1.01	63.6% 5p^2(^{3}P)5d ^{4}F + 11.0% 5p^2(^{3}P)5d ^{4}D
85 591.83	85 477	1.50	1.50	1.00	72.3% 5p^2(^{3}P)6s ^{4}P + 17.6% 5p^2(^{1}D)6s ^{2}D
87 404.54	87 546	1.26	1.25	1.00	36.6% 5s5p^4(^{1}D) ^{2}D + 32.6% 5p^2(^{1}D)5d ^{2}D
88 924.81	88 852	0.94	0.94	1.00	36.5% 5p^2(^{3}P)5d ^{2}F + 35.6% 5p^2(^{1}D)5d ^{2}F
92 793.22	92 782	1.25	1.24	1.01	50.6% 5p^2(^{3}P)5d ^{4}D + 12.2% 5p^2(^{3}P)5d ^{2}F
94 860.63	95 016	1.26	1.27	0.99	74.1% 5p^2(^{1}D)6s ^{2}D + 15.9% 5p^2(^{3}P)6s ^{4}P
99 229.68	99 054	1.53	1.51	1.01	64.7% 5p^2(^{3}P)5d ^{4}P + 10.1% 5s5p^4(^{3}P) ^{4}P
102 703.5	102 788	1.07	1.12	0.96	43.1% 5p^2(^{3}P)5d ^{2}D + 21.0% 5p^2(^{1}D)5d ^{2}F
108 819.4	108 578	1.03			33.6% 5p^2(^{3}P)5d ^{2}D + 26.1% 5p^2(^{1}D)5d ^{2}F
113 564.5	113 272	1.21			50.3% 5p^2(^{1}D)5d ^{2}D + 20.7% 5s5p^4(^{1}D) ^{2}D
116 837.31	116 886	1.21	1.20	1.01	30.9% 5p^2(^{3}P)6d ^{4}F + 15.0% 5p^2(^{3}P)6d ^{4}P
118 420.6	118 358	1.19			64.0% 5p^2(^{1}S)5d ^{2}D + 8.2% 5s5p^4(^{1}D) ^{2}D
120 617.13	120 516	1.51	1.51	1.00	75.5% 5p^2(^{3}P)7s ^{4}P + 18.5% 5p^2(^{1}D)7s ^{2}D
121 063.80	121 030	1.20	1.2	1.00	49.8% 5p^2(^{3}P)6d ^{4}F + 24.4% 5p^2(^{3}P)6d ^{4}P
122 196.84	122 057	1.06	1.07	0.99	59.4% 5p^2(^{3}P)6d ^{2}F + 19.1% 5p^2(^{3}P)6d ^{4}P

Notes. [(a)] Kramida et al. (2012). [(b)] HFR + CPOL (this work).

Table 5. continued.

E_{Exp}[a] (cm^{-1})	E_{Calc}[b] (cm^{-1})	g_{Calc}[b]	g_{Exp}[a]	g_{Calc}/g_{Exp}	LS-composition[b]
$J = 5/2$					
124 646.39	124 563	1.33	1.32	1.01	45.9% 5p^2(^{3}P)6d ^{4}D + 20.9% 5p^2(^{3}P)6d ^{4}P
125 906.03	125 815	1.15	1.17	0.98	41.5% 5p^2(^{3}P)6d ^{2}D + 17.5% 5p^2(^{1}D)6d ^{2}F
128 348.0	128 045	1.21			33.7% 5p^2(^{3}P)7d ^{4}F + 27.6% 5p^2(^{3}P)7d ^{4}D
129 897.22	129 742	1.28	1.29	0.99	76.6% 5p^2(^{1}D)7s ^{2}D + 20.0% 5p^2(^{3}P)7d ^{4}P
133 904.7	134 296	1.07			38.2% 5p^2(^{3}P)7d ^{2}D + 34.1% 5p^2(^{1}D)6d ^{2}F
135 093.1	135 152	1.20			46.1% 5p^2(^{1}D)6d ^{2}D + 11.6% 5p^2(^{3}P)7d ^{4}D
136 881.7	137 065	1.10			27.1% 5p^2(^{3}P)7d ^{2}D + 15.6% 5p^2(^{3}P)6d ^{2}D
147 870.1	147 386	1.19			87.7% 5p^2(^{1}S)6d ^{2}D + 2.2% 5p^2(^{3}P)6d ^{2}F
$J = 7/2$					
87 899.86	88 226	1.27	1.26	1.00	78.2% 5p^2(^{3}P)5d ^{4}F + 16.7% 5p^2(^{3}P)5d ^{4}D
90 797.21	90 677	1.25	1.25	1.00	35.0% 5p^2(^{3}P)5d ^{4}D + 30.9% 5p^2(^{1}D)5d ^{2}F
96 534.6	96 570	1.25	1.24	1.01	41.9% 5p^2(^{3}P)5d ^{4}D + 28.6% 5p^2(^{3}P)5d ^{2}F
100 835.8	100 736	0.97	0.98	0.99	71.5% 5p^2(^{1}D)5d ^{2}G + 22.7% 5p^2(^{1}D)5d ^{2}F
107 244.4	107 304	1.12	1.19	0.94	46.0% 5p^2(^{3}P)5d ^{2}F + 29.8% 5p^2(^{1}D)5d ^{2}F
120 667.5	120 673	1.29			59.2% 5p^2(^{3}P)6d ^{4}F + 30.5% 5p^2(^{3}P)6d ^{4}D
123 654.56	123 770	1.27	1.26	1.01	37.2% 5p^2(^{3}P)6d ^{4}D + 29.0% 5p^2(^{3}P)6d ^{4}F
125 967.10	125 807	1.15	1.15	1.00	57.4% 5p^2(^{3}P)6d ^{2}F + 15.5% 5p^2(^{3}P)6d ^{4}D
133 042.0	132 792	1.19			58.9% 5p^2(^{1}D)6d ^{2}F + 11.2% 5p^2(^{3}P)6d ^{4}D
133 769.00	133 682	1.04	1.04	1.00	59.6% 5p^2(^{1}D)6d ^{2}G + 16.6% 5p^2(^{3}P)7d ^{4}D
$J = 9/2$					
90 519.67	90 875	1.31	1.31	1.00	86.2% 5p^2(^{3}P)5d ^{4}F + 11.2% 5p^2(^{1}D)5d ^{2}G
	102 262	1.14			87.0% 5p^2(^{1}D)5d ^{2}G + 11.0% 5p^2(^{3}P)5d ^{4}F
123 649.92	123 705	1.30	1.30	1.00	80.8% 5p^2(^{3}P)6d ^{4}F + 16.0% 5p^2(^{1}D)5d ^{2}G

Table 6. Comparison between experimental and HFR+CPOL level energies and Landé factors in Te III (even levels).

E_{Exp}[a] (cm^{-1})	E_{Calc}[b] (cm^{-1})	g_{Exp}[c]	g_{Calc}[a]	g_{Calc}/g_{Exp}	LS-composition[b]
$J = 0$					
0.0	0				90.4% 5p^2 ^{3}P + 6.5% 5p^2 ^{1}S
30 398.3	30 398				88.1% 5p^2 ^{1}S + 6.6% 5p^2 ^{3}P
132 262.4	132 175				86.9% 5p6p ^{3}P + 10.0% 5p6p ^{1}S
$J = 1$					
4757.2	4767		1.50		96.9% 5p^2 ^{3}P + 1.0% 5s5p^2(^{1}D)5d ^{3}P
128 617.9	128 783	0.68	0.72	1.05	60.4% 5p6p ^{3}D + 33.9% 5p6p ^{1}P
132 116.7	131 959	1.24	1.30	1.05	44.9% 5p6p ^{3}P + 18.7% 5p6p ^{1}P
138 289.7	138 214	1.02	1.13	1.11	42.0% 5p6p ^{3}P + 36.8% 5p6p ^{1}P
141 803.0	141 692	1.76	1.86	1.06	79.6% 5p6p ^{3}S + 9.7% 5p6p ^{3}P
$J = 2$					
8167.0	8153		1.39		75.8% 5p^2 ^{3}P + 20.9% 5p^2 ^{1}D
17 359.8	17 364		1.11		75.3% 5p^2 ^{1}D + 20.9% 5p^2 ^{3}P
132 329.1	132 401	1.16	1.20	1.03	67.9% 5p6p ^{3}D + 15.1% 5p6p ^{3}P
139 664.5	139 611	1.43	1.37	0.96	62.1% 5p6p ^{3}P + 25.7% 5p6p ^{3}D
142 982.0	143 212	1.14	1.11	0.97	74.2% 5p6p ^{1}D + 19.5% 5p6p ^{3}P
$J = 3$					
139 949.7	139 970	1.28	1.33	1.04	96.2% 5p6p ^{3}D + 1.1% 5p4f ^{3}D

Notes. [(a)] The 5p^2 levels are taken from Tauheed & Naz (2011) and the 5p6p levels are from Kramida et al. (2012). [(b)] HFR + CPOL (this work). [(c)] Kramida et al. (2012).

values. Discarding these lines, we obtain a ratio of 1.07 ± 0.31. For these transitions, the MCDHF transition probabilities prove to have poorly converged; this is illustrated in Fig. 3 where the A-values in both gauges (circles and squares for Babushkin and Coulomb gauges) of one of the problematic transitions (5s^{2}5p^2 ^{3}P$_1$–5s^{2}5p6s ^{1}P$^o_1$) along with those of a converged transition (5s^{2}5p^2 ^{3}P$_2$–5s^{2}5p6s ^{3}P$^o_1$; diamonds for Babushkin and triangles for Coulomb) are plotted as a function of the calculation step. More correlation orbitals in the active set are clearly needed to stabilize these particular A-values but these calculations were not undertaken in the present work.

5. Conclusions

A first set of transition probabilities has been obtained for 439 transitions of Te II in the spectral range between 77 and 997 nm and for 284 transitions of Te III in the range 52–901 nm. Their accuracy has been assessed through the

Table 7. Comparison between experimental and HFR+CPOL level energies and Landé factors in Te III (odd levels).

E_{Exp}[a] (cm^{-1})	E_{Calc}[b] (cm^{-1})	g_{Exp}[b]	g_{Calc}[c]	g_{Calc}/g_{Exp}	LS-composition[b]
$J = 0$					
96 061.6	96 252				78.4% 5s5p^3(^{2}P) ^{3}P° + 18.1% 5p5d ^{3}P°
107 470.0	107 325				95.5% 5p6s ^{3}P° + 1.5% 5p^3(^{2}P)6s ^{3}P°
122 541.0	122 457				77.5% 5p5d ^{3}P° + 17.6% 5s5p^3(^{2}P) ^{3}P°
160 940.7	160 923				99.7% 5p7s ^{3}P° + 0.1% 5p6d ^{3}P°
172 389.2	172 347				95.7% 5p6d ^{3}P° + 1.8% 5p^3(^{2}P)6d ^{3}P°
184 537.3	184 527				99.9% 5p8s ^{3}P°
194 253.9	194 360				98.8% 5p7d ^{3}P° + 0.5% 5s5p^2(^{3}P)6p ^{3}P°
$J = 1$					
82 889.1	82 867		0.59		72.5% 5s5p^3(^{2}D) ^{3}D° + 14.6% 5p5d ^{3}D°
96 581.5	96 665		1.43		69.2% 5s5p^3(^{2}P) ^{3}P° + 17.1% 5p5d ^{3}P°
107 726.6	107 876	1.37	1.38	1.00	71.1% 5p6s ^{3}P° + 22.9% 5p6s ^{1}P°
114 216.4	114 186	1.00	1.63	1.63	57.3% 5s5p^3(^{4}S) ^{3}S° + 20.8% 5s5p^3(^{2}P) ^{1}P°
115 747.6	115 561		1.02		26.4% 5p6s ^{1}P° + 21.7% 5p5d ^{3}D°
117 796.1	118 010	1.26	0.95	0.75	35.1% 5p5d ^{3}D° + 29.9% 5p6s ^{1}P°
122 127.4	121 874		1.17		31.9% 5p5d ^{3}P° + 15.9% 5p5d ^{3}D°
124 787.9	124 725		1.33		26.5% 5p5d ^{3}P° + 23.1% 5p5d ^{1}P°
136 476.2	136 268		1.02		42.9% 5s5p^3(^{2}P) ^{1}P° + 39.6% 5p5d ^{1}P°
161 196.5	161 214	1.43	1.35	0.94	70.1% 5p7s ^{3}P° + 29.0% 5p7s ^{1}P°
163 334.2	163 237		0.76		62.4% 5p6d ^{3}D° + 16.8% 5p6d ^{1}P°
170 586.9	170 577		1.12		64.6% 5p7s ^{1}P° + 26.9% 5p7s ^{3}P°
172 159.0	172 100		1.28		71.4% 5p6d ^{3}P° + 19.5% 5p6d ^{3}D°
174 499.3	174 603		1.00		72.1% 5p6d ^{1}P° + 9.0 % 5p6d ^{3}D°
184 657.0	184 667		1.34		67.7% 5p8s ^{3}P° + 31.0% 5p8s ^{1}P°
185 501.0	185 469		0.81		55.4% 5p7d ^{3}D° + 24.6% 5p7d ^{1}P°
193 612.7	193 642		1.13		63.3% 5p8s ^{1}P° + 28.9% 5p8s ^{3}P°
194 446.8	194 294		1.28		60.8% 5p7d ^{3}P° + 21.8% 5p7d ^{3}D°
195 268.7	195 282		0.99		68.8% 5p7d ^{1}P° + 13.5% 5p7d ^{3}D°
$J = 2$					
64 586.5	64 560		1.98		95.0% 5s5p^3(^{4}S) ^{5}S° + 3.7% 5s5p^3(^{2}P) ^{3}P°
83 203.4	83 125		1.22		70.2% 5s5p^3(^{2}D) ^{3}D° + 13.6% 5p5d ^{3}D°
95 031.3	94 760		1.17		33.9% 5p5d ^{1}D° + 21.5% 5s5p^3(^{2}P) ^{3}P°
100 469.1	100 505	1.13	1.26	1.12	38.7% 5s5p^3(^{2}P) ^{3}P° + 26.4% 5p5d ^{1}D°
104 717.2	104 772		0.71		85.6% 5p5d ^{3}F° + 4.0% 5p5d ^{1}D°
115 422.2	115 513	1.28	1.47	1.15	75.6% 5p6s ^{3}P° + 8.7% 5p5d ^{3}D°
116 719.4	116 750	1.34	1.35	1.01	30.6% 5p5d ^{3}D° + 30.1% 5p5d ^{3}P°
122 515.0	122 440		1.25		40.2% 5p5d ^{3}D° + 24.5% 5p5d ^{3}P°
127 188.8	127 455		1.10		48.9% 5s5p^3(^{2}D) ^{1}D° + 25.6% 5p5d ^{1}D°
161 407.4	161 574		0.76		72.8% 5p6d ^{3}F° + 18.3% 5p6d ^{1}D°
162 745.6	162 602		1.26		38.9% 5p6d ^{3}P° + 36.3% 5p6d ^{3}D°
170 017.4	170 029		1.49		96.3% 5p7s ^{3}P° + 1.3% 5p6d ^{1}D°
170 417.2	170 612		0.98		45.8% 5p6d ^{1}D° + 27.6% 5p6d ^{3}D°
171 965.0	171 871		1.35		54.5% 5p6d ^{3}P° + 26.8% 5p6d ^{3}D°
184 408.8	184 588		0.76		75.8% 5p7d ^{3}F° + 18.1% 5p7d ^{1}D°
185 193.7	185 081		1.29		45.8% 5p7d ^{3}P° + 34.8% 5p7d ^{3}D°
193 414.9	193 397		1.49		96.6% 5p8s ^{3}P° + 1.4% 5p7d ^{3}P°
193 745.5	193 759		0.98		50.5% 5p7d ^{1}D° + 26.1% 5p7d ^{3}D°
194 349.2	194 214		1.33		50.5% 5p7d ^{3}P° + 32.1% 5p7d ^{3}D°
$J = 3$					
85 205.6	85 251		1.33		81.4% 5s5p^3(^{2}D) ^{3}D° + 15.6% 5p5d ^{3}D°
106 314.8	106 472	1.07	1.09	1.02	92.4% 5p5d ^{3}F° + 1.6% 5p^3(^{2}P)5d ^{3}F°
120 903.4	120 729	1.35	1.31	0.97	74.0% 5p5d ^{3}D° + 13.4% 5s5p^3(^{2}D) ^{3}D°
127 242.3	127 539		1.02		87.7% 5p5d ^{1}F° + 4.7% 5p5d ^{3}D°
162 776.6	162 844		1.13		53.0% 5p6d ^{3}F° + 24.1% 5p6d ^{3}D°
171 069.7	170 949		1.24		61.5% 5p6d ^{3}D° + 33.5% 5p6d ^{3}F°
173 220.2	173 245		1.04		75.0% 5p6d ^{1}F° + 9.9% 5p6d ^{3}D°
185 347.4	185 307		1.12		49.8% 5p7d ^{3}F° + 25.2% 5p7d ^{1}F°
193 930.5	193 899		1.24		60.4% 5p7d ^{3}D° + 37.1 5p7d ^{3}F°
194 800.0	194 932		1.06		71.9% 5p7d ^{1}F° + 14.6 5p7d ^{3}D°
$J = 4$					
	110 385		1.25		95.9% 5p5d ^{3}F° + 1.7% 5s5p^3(^{2}P)5d ^{3}F°

Notes. [(a)] Tauheed & Naz (2011). [(b)] HFR + CPOL (this work). [(c)] Kramida et al. (2012).

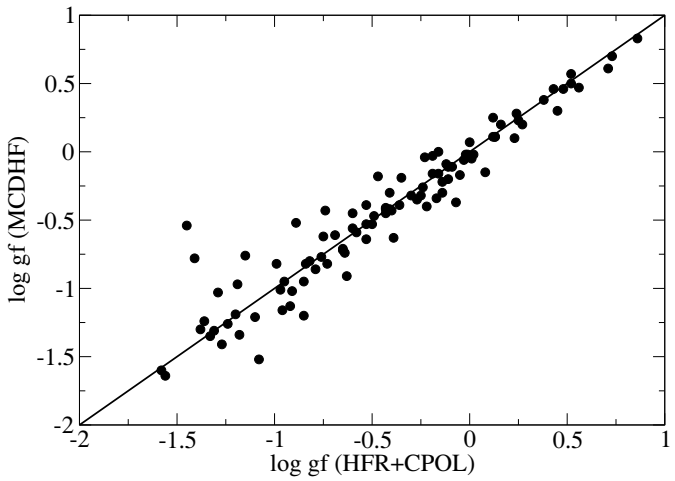

Fig. 1. Comparison between MCDHF and HFR+CPOL log gf in Te II. Transitions with $CF > 0.05$ and gauges agreements better than 10% have been retained. A straight line of equality has been drawn.

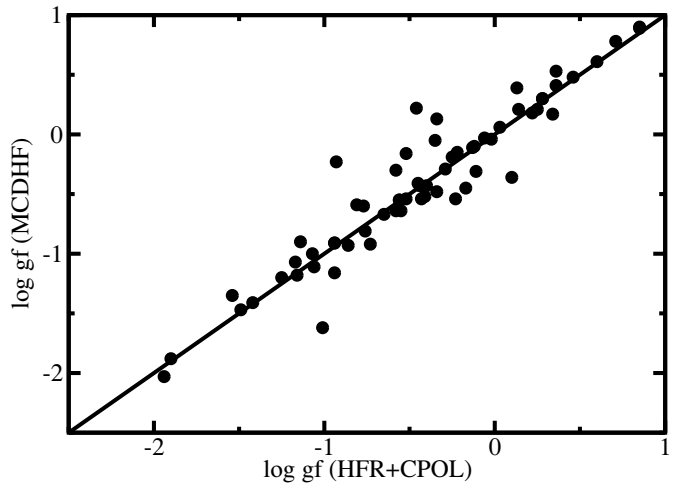

Fig. 2. Same as in Fig. 1 for Te III.

comparison of the results obtained by two independent theoretical approaches, i.e. the HFR+CPOL and the MCDHF approximations. The satisfying agreement which is observed indicates that the scale of f values is firmly established. This new set of results is expected to help the astrophysicists in the investigation of VUV high resolution spectra and hopefully will contribute to throw some light on nucleosynthesis processes regarding the production of heavy elements in metal-poor stars.

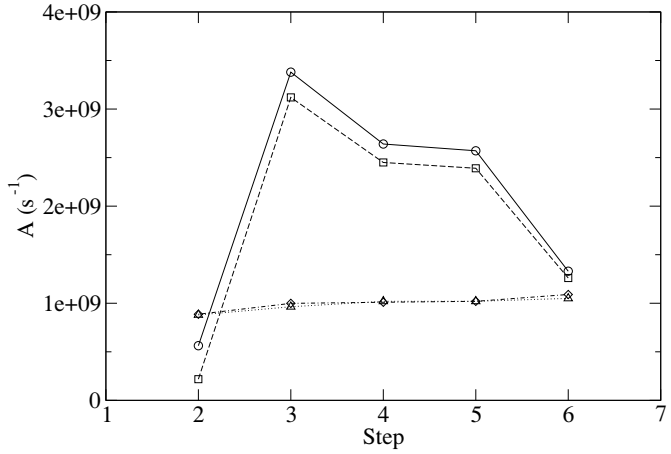

Fig. 3. A-values in both gauges (circles and squares for Babushkin and Coulomb gauges) of the $5s^25p^2\ ^3P_1-5s^25p6s\ ^1P^o_1$ transition in Te III along with those of $5s^25p^2\ ^3P_2-5s^25p6s\ ^3P^o_1$ transition in the same ion (diamonds for Babushkin and triangles for Coulomb) plotted as function of the calculation step. The first transition shows a convergence problem.

Acknowledgements. Financial support from the belgian FRS-FNRS is acknowledged. P.P., P.Q. and E.B. are respectively Research Associate, Research Director and Honorary Research Director of this organization.

References

Biémont, E., Hansen, J. E., Quinet, P., & Zeippen, C. J. 1995, A&AS, 111, 333
Cowan, R. D. 1981, The Theory of Atomic Structure and Spectra (Berkeley: University of California Press)
Cowley, C. H., Hartoog, M. R., Aller, M. F., & Cowley, A. P. 1973, ApJ, 183, 127
Crooker, A. M., & Joshi, Y. N. 1964, JOSA, 54 553
Eriksson, K. B. S. 1974, J. Opt. Soc. Am., 64, 1272
Grant, I. P. 1988, in Methods of Computational Chemistry, ed. S. Wilson (New York: Plenum Press), 2, 1
Handrup, M. B., & Mack, J. E. 1964, Physica (Utrecht), 30, 1245
Jonsson, P., He, X., Froese Fischer, C., & Grant, I. P. 2007, Comput. Phys. Commun., 177, 597
Joshi, Y. N., Tauheed, A., & Davison I. G. 1992, Can. J. Phys., 70, 740
Kramida, A., Ralchenko, Yu., Reader, J., and NIST ASD Team 2012, NIST Atomic Spectra Database (ver. 5.0), available: http://physics.nist.gov/asd, National Institute of Standards and Technology, Gaithersburg, MD
Krishnamurty, S. G., & Rao, K. R. 1937, Proc. R. Soc. London Ser. A, 158, 562
Roederer, I. U. , Lawler, J. E. , Cowan, J. J., et al. 2012, ApJ, 747, L8
Tauheed, A., Joshi, Y. N., & Steinitz, M. 2009, Can. J. Phys., 87, 1255
Tauheed, A., & Naz, A. 2011, J. Korean Phys. Soc., 59, 2910
Werel, K., & Augustyniak, L. 1981, Phys. Scr., 23, 856